IEEE Access
Multidisciplinary ⋮ Rapid Review ⋮ Open Access Journal

Received January 19, 2020, accepted February 5, 2020, date of publication February 10, 2020, date of current version February 18, 2020.

Digital Object Identifier 10.1109/ACCESS.2020.2972935

A Wavelet Threshold Denoising-Based Imbalance Fault Detection Method for Marine Current Turbines

ZHICHAO LI[1], TIANZHEN WANG[1], (Senior Member, IEEE), YIDE WANG[2], (Senior Member, IEEE), YASSINE AMIRAT[3], (Senior Member, IEEE), MOHAMED BENBOUZID[1,4], (Fellow, IEEE), AND DEMBA DIALLO[5], (Senior Member, IEEE)

[1]Logistics Engineering College, Shanghai Maritime University, Shanghai 201306, China
[2]Institut d'Electronique et de Telecommunications de Rennes (IETR), UMR, École Polytechnique de l'Université de Nantes, 44306 Nantes, France
[3]Department of Electrical Engineering, ISEN Yncréa Ouest, UMR CNRS 6027 IRDL, 29200 Brest, France
[4]FRE CNRS, Institut de Recherche Dupuy de Lôme (IRDL), University of Brest, 29238 Brest, France
[5]CNRS, CentraleSupelec, University Paris-Saclay, 91192 Gif-Sur-Yvette, France

Corresponding author: Tianzhen Wang (tzwang@shmtu.edu.cn)

This work was supported by the National Natural Science Foundation of China under Grant 61673260, and the Shanghai Natural Science Foundation under Grant 16ZR1414300.

ABSTRACT Blade imbalance fault caused by the marine organisms is considered as the most important fault in marine current turbines. Therefore, it is important to detect the fault accurately and quickly to mitigate its effect, minimize the downtime, and maximize the productivity. Imbalance fault detection methods using generator stator current signals have attracted attentions due to their low cost, operability and stability compared to the ones using vibration analysis. However, it is difficult to extract the fault signature and automatically detect the imbalance fault under different flow velocity conditions. In this paper, a wavelet threshold denoising-based imbalance fault detection method using the stator current is proposed. The signal is analyzed through three consecutive steps: the parameters offline setting based on wavelet threshold denoising, the Hilbert transform method and the Principle Component Analysis-based detection method. With this approach, the imbalance fault can be detected automatically. The imbalance fault detection is assessed under different flow velocity conditions and validated using an experimental platform. The results are promising with false alarm and false negative rates less than 1% and 5% respectively when using Q statistic. Moreover, the experimental results show that the proposed method has good stability under different flow velocity conditions.

INDEX TERMS Hilbert transform, imbalance fault, marine current turbine, principle component analysis, wavelet.

I. INTRODUCTION

In recent years, with the increasing energy consumption around the world and the sharp increase of environmental pollution, marine energy has attracted more and more attention around the world due to its high energy density, predictability and relative stability [1]–[3]. Marine current power generation is becoming more attractive and competitive [4], [5], and its technology has made great progress [6], as proved by the number of projects using marine current turbines (MCTs) [7]. It is foreseeable that MCTs will become more and more important in power supply systems [8]. However, the seabed environment is complex and MCTs installed under the sea will be considered as artificial reefs and attract a variety of marine organisms which will lead to imbalance faults [9], [10]. The imbalance faults will affect the operation of the system, which not only degrades the performance of MCTs, but may also significantly damage its structure [11]. In addition, the MCT installed under water is affected by many factors such as attachments, surges, turbulence, etc. And it is difficult to extract the imbalance fault signature [12]. To improve both the safety and reliability of MCT systems, it is necessary to find an effective technology to complete the imbalance fault detection in MCTs [13].

To detect the imbalance fault, methods using sensors are proposed and good detection results are obtained [14], [15].

The associate editor coordinating the review of this manuscript and approving it for publication was Ruqiang Yan.

However, the fault detection using stator current signals has many advantages because it costs less and does not need to consider sensors faults [16]. To reduce the interferences caused by turbulence and waves, different methods are proposed. The empirical mode decomposition (EMD) method is used to decompose the stator current signal into different intrinsic mode functions (IMFs) and extract the IMF containing the fault signature to detect the imbalance fault [17]–[19]. In [20] and [21], the moving average filter method is used to filter the interference in the signal. All these methods contribute to the denoising of the stator current signal measured from the MCT system and the imbalance fault detection. However, for the strategies using EMD, there are still some problems such as the end effect and the modal confusion [22]; for the strategies using the moving average filter method, only the high frequency signals can be filtered. As reported in [23], the wavelet transform method is used to preprocess the raw signal, reduce the interference components and extract the useful information to detect the fault. However, it is difficult for these methods using wavelet transform to set the appropriate parameters in practical application. In order to decrease the data dimensions and automatically detect the fault, the Principle Component Analysis (PCA) is used in [24] and [25]. With this method, a standard model in healthy state can be built, and the fault can be detected automatically. However, the PCA method could not be directly applied to the imbalance fault detection because data preprocessing is required.

All of the above methods have made great contributions to the fault detection, but the continuously changing flow velocity has not been fully considered. The fault characteristic frequency is not constant and changes with the flow velocity [26], [27], which will lead to different fault characteristic frequencies at different times. However, the main objective of the existing imbalance fault detection methods is to highlight the fault characteristic frequency, which means that the stability of these methods needs to be improved under different flow velocity conditions.

A. PAPER CONTRIBUTIONS

To reduce the interference and detect the imbalance fault under different flow velocity conditions, a wavelet threshold denoising-based imbalance fault detection method for MCTs is proposed. The proposed approach contains three parts: the parameters offline setting based on wavelet threshold denoising, the Hilbert transform (HT) method and the PCA-based detection method. With this method, the imbalance fault of MCTs can be detected automatically. The experimental results indicate that the proposed method gives good detection results under different flow velocity conditions. Table 1 shows the advantages of the proposed method compared with some of the present methods.

B. PAPER STRUCTURE

The structure of this paper is as follows. In Section 2, the problem in the imbalance fault detection is described.

TABLE 1. The advantages of the proposed method compared with present methods.

	Method in [18]	Method in [20]	Method in [27]	Proposed method
Extract the fault signature?	Yes	Yes	Yes	Yes
Consider the influence of turbulence and waves?	Yes	Yes	Yes	Yes
The stability under different flow velocity conditions.	**Not good**	**Not good**	**Not good**	**Good**
Detect the fault automatically?	**No**	**No**	**No**	**Yes**

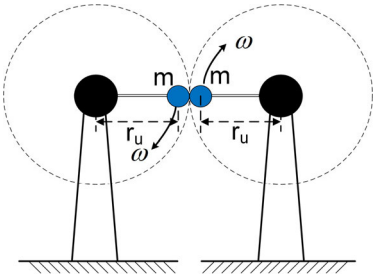

FIGURE 1. The effect of blade imbalance in an MCT [20].

In Section 3, the proposed wavelet threshold denoising-based imbalance fault detection method is introduced. In Section 4, experimental results are given to verify the effectiveness of the proposed method. Finally, conclusion in Section 5 closes the paper.

II. PROBLEM DESCRIPTION

This paper mainly considers the direct-drive permanent magnet synchronous generator (PMSG) MCT which is gaining more and more acceptances. The motion equation of a direct-drive PMSG MCT can be expressed as follows [20]:

$$J\frac{d\omega_r(t)}{dt} = T_t(t) - T_e(t) - D\omega_r(t) \quad (1)$$

$$\omega_r(t) = 2\pi f_r(t) \quad (2)$$

where J denotes the total inertia constant, ω_r denotes the angular speed of the shaft, $d\omega_r(t)/dt$ denotes the angular acceleration, T_t and T_e are the turbine torque and the generator torque, respectively. D denotes the damping coefficient, f_r denotes the shaft rotating frequency (1P frequency) which changes with the flow velocity. If an imbalance fault happens, an excitation will appear in the frequency domain of the angular speed signal with the same frequency as 1P frequency [26]. Therefore, the shaft rotating frequency f_r can be used as the fault signature.

When an imbalance fault occurs on a blade, its mass distribution will be different from the others. An equivalent imbalance mass will occur and induce a vibration in the shaft rotating speed. As shown in Fig. 1, m denotes the equivalent imbalance mass, and r_u denotes the distance between the imbalance mass and the shaft. Both m and r_u can affect the

torque on the shaft, and the torque distortion caused by a bigger m and a smaller r_u may be equal to that caused by a smaller m and a bigger r_u. To analyze the imbalance fault, r_u is set constant in this paper.

In a direct-drive PMSG MCT, the stator current can be expressed as:

$$i_s(t) = I_s \cos(p\omega_r t + \gamma) \tag{3}$$

where I_s is the current amplitude, p is the number of pole pairs, γ is the initial angle. In this case, the stator current frequency is $f_e = (p\omega_r)/(2\pi)$. The f_e is given as follows:

$$f_e(t) = pf_r(t) \tag{4}$$

The fault information in the shaft rotation frequency can be transferred to the instantaneous frequency of the stator current signal. Therefore, it is difficult to find the fault information in time domain. Fig. 2 shows the stator current signals recorded from an MCT in different health states. Fig. 2(a) is the current signal in the healthy state and Fig. 2(b) is in the imbalance fault state. In time domain, the stator signals in different health states are almost the same.

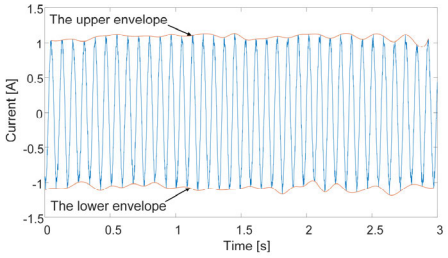

(a) In the healthy state.

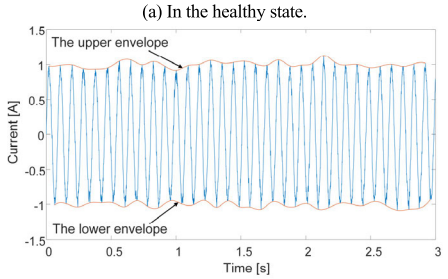

(b) In the imbalance fault state.

FIGURE 2. The stator current signals of the MCT in different health states.

With the instantaneous frequency, the imbalance fault signature can be extracted, which means that the fault can be detected in time-frequency domain (the instantaneous frequencies in different health states are shown in Section 4).

The imbalance fault signature comes from the torque distortion on the turbine [27]. However, in marine environment, the turbulence and waves will bring interferences to the stator current signal [28]. In recent years, researchers have proposed some methods or strategies to reduce the interference and extract the imbalance fault signature. The methods proposed in [18] and [26] use the EMD to decompose the raw signal into IMFs. The EMD method can reduce the interference information, which is caused by environmental factors. And the imbalance fault can be detected in one of the IMFs. The method in [20] uses the moving average filter which can be regarded as a low-pass filter to reduce the interference information and can get a good denoising performance. However, these methods do not consider the influences of different flow velocity conditions. And the imbalance fault is detected by searching the fault peak near the fault characteristic frequency, which means that the detection results will be influenced by the shaft rotation frequency. In actual MCT systems, the flow velocity is always changing [29], which means that the shaft rotation frequency takes on different values over time. The fault characteristic frequencies in the same fault state under different flow velocity conditions are shown in Fig. 3. It can be observed that the fault characteristic frequencies are different under different flow velocity conditions. Therefore, it is difficult to set a detection limit to automatically detect the imbalance fault. Moreover, the interferences caused by the turbulence and waves changes with the flow velocity. When using EMD, the relevant IMF selection is tricky under different flow velocity conditions. For the moving average filter method, it can only filter out the high frequency signals, but cannot extract the signal in specific frequency band. Therefore, the stability of the methods mentioned above under different flow velocity conditions needs to be improved.

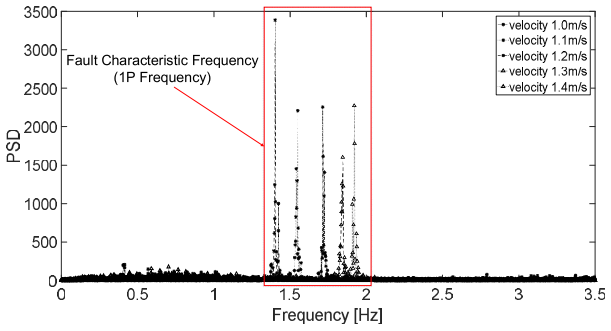

FIGURE 3. The MCT's fault characteristic frequencies in imbalance fault state under different flow velocity conditions.

III. THE WAVELET THRESHOLD DENOISING-BASED IMBALANCE FAULT DETECTION METHOD

To address the problems mentioned above, a wavelet threshold denoising-based imbalance fault detection method for MCTs is proposed. It is composed of three parts: the parameters offline setting based on wavelet threshold denoising, the HT method and the PCA-based detection method. The proposed method can automatically detect the imbalance fault and has good stability under different flow velocity conditions. Moreover, anyone of the three-phase stator current signals can be used in this method. This means that if one of the three-phase stator current signals cannot be used due to some other faults, this method can still detect the imbalance fault. It makes this approach attractive for implementation [30].

A. PARAMETERS OFFLINE SETTING BASED ON WAVELET THRESHOLD DENOISING

To reduce the interference in the stator current signal under different flow velocity conditions, the wavelet threshold denoising method is used. As it is difficult to choose the parameters of the method using wavelet decomposition [31], an offline parameters' setting is proposed.

In the application of fault detection for MCTs, the acquired signals are usually non stationary. In the signal, there may be some peaks or abrupt parts caused by the interference which can be regarded as noise. The wavelet threshold denoising method can be used to preprocess the signal and reduce the interference. The signal model of the stator current is as follows:

$$x(n) = y(n) + e(n), \quad n = 1, 2, \cdots, N \tag{5}$$

where $x(n)$ denotes the signal with noise, N denotes the length of the signal, $y(n)$ denotes the signal without noise, $e(n)$ represents the noise. In discrete wavelet transform (DWT), $x(n)$ is processed through a series of filters with different characteristic frequencies.

By thresholding the wavelet coefficients which represent the noise, the interference in the signal can be reduced. The process of the wavelet threshold denoising is as follows:

a) Set the wavelet basis and the number of decomposition levels.
b) Use DWT to decompose the signal.
c) Use the thresholding function and the calculated threshold to get the filtered wavelet coefficients.
d) Reconstruct the signal with the approximated and filtered wavelet coefficients.

In the wavelet threshold denoising method, the number of decomposition levels, the wavelet basis function and the threshold selection function are important factors which can influence the denoising performance [32]. To set suitable parameters, an offline method with two steps is proposed: the setting of the number of decomposition levels, and the setting of the wavelet basis function and the threshold selection function. This method is implemented offline with historical data of the MCT in healthy state.

1) SETTING OF THE NUMBER OF DECOMPOSITION LEVELS

The frequency range after wavelet decomposition is related to the sampling frequency F_s of the historical data $x(n)$. If the number of the decomposition levels is j, the corresponding bandwidth of the smallest band is $B_j = F_s/2^{j+1}$. In the actual imbalance fault detection of MCTs, usually only the first or second harmonic of the electrical signal is needed [26]. Therefore, to achieve better fault detection, the bandwidth of the smallest band should satisfy:

$$B_j \geq 2f \tag{6}$$

where f denotes the average frequency of the stator current. Substitute B_j in (6), the number of decomposition levels can be represented as $j \leq \log_2[F_s/(4f)]$. To make the useful information clear and minimize the calculation time of the wavelet decomposition process, the number of decomposition levels is set as:

$$j = \left\lfloor \log_2\left(\frac{F_s}{4f}\right) \right\rfloor \tag{7}$$

where $\lfloor * \rfloor$ indicates that the $*$ is rounded down.

2) SETTING OF THE WAVELET BASIS FUNCTION AND THE THRESHOLD SELECTION FUNCTION

To set the wavelet basis function and the threshold selection function, different parameters are used in the offline setting method to denoise the historical data $x(n)$. Four wavelet basis functions (Haar, Db4, Coif4, Sym4) and four threshold selection functions (sqtwolog, rigrsure, heursure, minimaxi) are used in this paper. In order to evaluate the denoising performance of different parameter groups, the signal to noise ratio (SNR), the mean square error (MSE) and the correlation coefficient (CORR) are used in this paper [33].

The SNR is a traditional parameter which can reflect the ratio of signal to noise. The amount of the noise removed can be reflected by this parameter. The SNR_i of the denoising result with the ith ($i = 1, 2, 3, \cdots, I$, I denotes the total number of the parameter groups) parameter group can be defined as:

$$SNR_i = 10\log_{10}\left(\frac{\frac{1}{N}\sum_{n=1}^{N} Y_i^2(n)}{\frac{1}{N}\sum_{n=1}^{N}[x(n) - Y_i(n)]^2}\right) \tag{8}$$

where $Y_i(n)$ is the denoising results with the ith parameter group. Therefore, the smaller the SNR is, the larger the noise is removed. The MSE can reflect the error between the original and the denoised signals. It can be defined as follows:

$$MSE_i = \frac{1}{N}\sum_{n=1}^{N}(x(n) - Y_i(n))^2 \tag{9}$$

where MSE_i indicates the MSE of the denoising result with the ith parameter group. The smaller the MSE is, the more similar the denoised signal is to the original one. The CORR is a criterion which can reflect the correlation of signals before and after denoising. The $CORR_i$ of the denoising result with the ith parameter group can be defined as follows:

$$CORR_i = \frac{\sum_{n=1}^{N}(x(n) - \overline{x})\left(Y_i(n) - \overline{Y}_i\right)}{\sqrt{\sum_{n=1}^{N}(x(n) - \overline{x})^2}\sqrt{\sum_{n=1}^{N}\left(Y_i(n) - \overline{Y}_i\right)^2}} \tag{10}$$

where $\overline{x}$ and $\overline{Y}_i$ are the averages of $x(n)$ and $Y_i(n)$, respectively. By using these three criteria, the denoising performance can be measured. The best denoising result should satisfy these following conditions: the smallest SNR, the smallest MSE and the largest CORR. The suitable parameter group is set by comparing the denoising performance of different parameter groups. The suitable parameter group corresponding to each kind of evaluation criteria can be determined by:

$$[M_{\text{snr}}, i_{\text{snr}}] = \min(SNR_i) \tag{11}$$

$$[M_{\text{mse}}, i_{\text{mse}}] = \min(MSE_i) \tag{12}$$

$$[M_{\text{corr}}, i_{\text{corr}}] = \max(CORR_i) \tag{13}$$

where M_{snr}, M_{mse} and M_{corr} denote the best values of different evaluation criteria. In practical, the denoising results may not satisfy the above conditions at the same time (the i_{snr}th, the i_{mse}th and the i_{corr}th parameter groups may not be the same group). Therefore, in this proposed method, the parameter group satisfying as many optimal conditions as possible is set.

There are three situations in the relationship between i_{snr}, i_{mse} and i_{corr}. When i_{snr}, i_{mse} and i_{corr} are all different, the i_{corr}th parameter group is selected to ensure that there is enough useful information in the denoised signal. When two of i_{snr}, i_{mse} and i_{corr} are the same (assuming the value is a), the ath parameter group is selected. When i_{snr}, i_{mse} and i_{corr} are all the same (assuming the value is b), the bth parameter group is selected. All the situations are summarized in Table 2.

TABLE 2. Parameter group setting rules.

Different situations	Parameter group setting results
$i_{\text{snr}} \neq i_{\text{mse}} \neq i_{\text{corr}}$	The i_{corr} th parameter group should be set as the final group to ensure that enough information is retained in the denoised signal.
$a = i_{\text{snr}} = i_{\text{mse}} \neq i_{\text{corr}}$ or $a = i_{\text{snr}} = i_{\text{corr}} \neq i_{\text{mse}}$ or $a = i_{\text{mse}} = i_{\text{corr}} \neq i_{\text{snr}}$	The a th parameter group is selected.
$b = i_{\text{snr}} = i_{\text{mse}} = i_{\text{corr}}$	The b th parameter group is selected.

B. HILBERT TRANSFORM

After the parameters offline setting based on wavelet threshold denoising, the HT is used [34]. By using the HT, the stator current signal is transformed from time domain to time-frequency domain. The HT of the denoised stator current $Y(t)$, denoted by $h(t)$, can be defined as:

$$h(t) = H[Y(t)] = \frac{1}{\pi}\int_{-\infty}^{\infty}\frac{Y(t)}{t-\tau}d\tau \tag{14}$$

The HT is actually the convolution of $Y(t)$ with $1/t$. The complex conjugate pair formed by $Y(t)$ and $h(t)$ can be given as:

$$z(t) = Y(t) + jh(t) = A(t)\,e^{j\phi(t)} \tag{15}$$

In this case, the amplitude $A(t)$ and the phase $\phi(t)$ are given respectively by:

$$A(t) = |z(t)| = \sqrt{Y^2(t) + h^2(t)} \tag{16}$$

$$\phi(t) = \arctan\left[\frac{h(t)}{Y(t)}\right] \tag{17}$$

The instantaneous frequency of $Y(t)$ can be computed by:

$$f_{\text{e}}(t) = \frac{1}{2\pi}\frac{d\phi(t)}{dt} \tag{18}$$

The estimated stator current instantaneous frequency f_{e} can be used as the imbalance fault signature. After the frequency domain analysis, the frequency domain signal $s(k)$ (where k is the number of the frequency bands) of f_{e} can be used to detect the imbalance fault in MCTs.

C. PCA-BASED DETECTION

To reduce data dimensions and automatically detect the imbalance fault in MCTs, a PCA-based detection method [35] is used in this paper. By using PCA, the dimensions of the frequency domain signal are reduced and the reference model influenced by the turbulence and waves is established. Then, the statistics and the control limits are calculated.

The PCA-based detection method consists of three parts:

1) DATA NORMALIZATION

Before building the PCA model, the frequency domain signal $s(k)$ is preprocessed. Compose all the signals $s(k)$ obtained under different flow velocity conditions into matrix $\boldsymbol{S} \in \boldsymbol{R}^{q\times k}$ (q is the number of samples). Normalize the S by z-score method:

$$\boldsymbol{S}^* = \frac{\boldsymbol{S} - \overline{\boldsymbol{S}}}{\sqrt{\text{Var}(\boldsymbol{S})}} \tag{19}$$

where $\overline{\boldsymbol{S}}$ and $\text{Var}(\boldsymbol{S})$ are the mean and variance of S, respectively.

2) DATA MATRIX MODEL

The normalized data set $\boldsymbol{S}^*$ can be expressed as:

$$\boldsymbol{S}^* = \boldsymbol{T}\boldsymbol{P}^{\text{T}} \tag{20}$$

where matrix $\boldsymbol{T} = [\boldsymbol{t}_1, \boldsymbol{t}_2, \cdots, \boldsymbol{t}_k] \in \mathbf{R}^{q\times k}$ contains the transformed variables, $\boldsymbol{t}_i \in \mathbf{R}^q$ are the principal components (PCs), matrix $\boldsymbol{P} = [\boldsymbol{p}_1, \boldsymbol{p}_2, \cdots, \boldsymbol{p}_k] \in \mathbf{R}^{k\times k}$ contains the orthogonal vectors $\boldsymbol{p}_i \in \mathbf{R}^k$. $\boldsymbol{C}$ is a covariance matrix and it can be expressed as follows:

$$\boldsymbol{C} = \boldsymbol{S}^{*T}\boldsymbol{S}^*/(q-1) = \boldsymbol{P}\boldsymbol{\Lambda}\boldsymbol{P}^{\text{T}} \tag{21}$$

where $\boldsymbol{P}\boldsymbol{P}^{\text{T}} = \boldsymbol{P}^{\text{T}}\boldsymbol{P} = \boldsymbol{I}_k$, the diagonal matrix $\boldsymbol{\Lambda} = \text{diag}\{\lambda_1, \lambda_2, \cdots, \lambda_k\}$ ($\lambda_1 \geq \lambda_2 \geq \cdots \geq \lambda_k$) contains the eigenvalues corresponding to the k PCs, $\boldsymbol{I}_k$ is the identity matrix. To reduce the computation, the number of PCs (l) need to be smaller. To choose the l, Cumulative Percent Variance (CPV) is used in this paper and it can be computed as:

$$CPV(l) = \frac{\sum_{i=1}^{l}\lambda_i}{\sum_{i=1}^{k}\lambda_i} \times 100\% \tag{22}$$

Then the matrix $\boldsymbol{S}^*$ can be expressed as:

$$\boldsymbol{S}^* = \boldsymbol{T}\boldsymbol{P} = \left[\hat{\boldsymbol{T}}\tilde{\boldsymbol{T}}\right]\left[\hat{\boldsymbol{P}}\tilde{\boldsymbol{P}}\right]^{\text{T}} \tag{23}$$

where matrices $\hat{\boldsymbol{T}} \in \mathbf{R}^{q\times l}$ and $\tilde{\boldsymbol{T}} \in \mathbf{R}^{q\times(k-l)}$ contain l retained PCs and $k-l$ PCs, respectively. Matrices $\hat{\boldsymbol{P}} \in \mathbf{R}^{q\times l}$

and $\tilde{\boldsymbol{P}} \in \mathbf{R}^{q\times(k-l)}$ contain l retained eigenvectors and $k-l$ eigenvectors respectively. Then (23) can be expressed as:

$$\begin{aligned}\boldsymbol{S}^* &= \hat{\boldsymbol{T}}\hat{\boldsymbol{P}}^{\mathrm{T}} + \tilde{\boldsymbol{T}}\tilde{\boldsymbol{P}}^{\mathrm{T}} \\ &= \boldsymbol{S}^*\hat{\boldsymbol{P}}\hat{\boldsymbol{P}}^{\mathrm{T}} + \boldsymbol{S}^*\left(\boldsymbol{I}_k - \hat{\boldsymbol{P}}\tilde{\boldsymbol{P}}^{\mathrm{T}}\right) \\ &= \hat{\boldsymbol{S}}^* + \tilde{\boldsymbol{S}}^* \end{aligned} \tag{24}$$

where $\hat{\boldsymbol{S}}^*$ represents the projection of $\boldsymbol{S}^*$ in the principal subspace, and $\tilde{\boldsymbol{S}}^*$ in the residual subspace.

3) SAMPLE STATISTICS AND CONTROL LIMIT

In the constructed PCA model, the interferences caused by the turbulence and waves are considered. To detect the imbalance fault in MCTs, two fault detection indices are used in this paper: the T^2 statistic and the Q statistic [36]. The T^2 statistic represents the changes in the principal subspace, and the Q statistic represents the changes in the residual subspace. T^2 statistic and Q statistic can be expressed as:

$$T^2 = ||\boldsymbol{S}^*||_2^2 = \boldsymbol{S}^{*T}\boldsymbol{P}\boldsymbol{\Lambda}^{-1}\boldsymbol{P}^{\mathrm{T}}\boldsymbol{S}^* \le \mathrm{T}_\alpha^2 \tag{25}$$

$$Q = ||\tilde{\boldsymbol{S}}^*||_2^2 \le \delta_\alpha^2 \tag{26}$$

where T_α^2 and δ_α^2 are the limits for the T^2 statistic and Q statistic, respectively. If the statistic exceeds its upper limit, it is assumed that a fault has occurred.

D. THE PROPOSED IMBALANCE FAULT DETECTION METHOD

The proposed imbalance fault detection method is done in two parts: offline training part and online detecting part. In the offline training part, using the historical data of the healthy MCT's stator current, the parameters of the wavelet threshold denoising method are set and the healthy MCT reference model is established. In the online detecting part, the former parameters are used to reduce the interference in the newly measured stator current signal. And after the HT and PCA, the data is projected into the reference model space, where the statistical fault indices can be computed in the principal or the residual subspace, to make the decision. The flowchart in Fig. 4 summarizes the procedure.

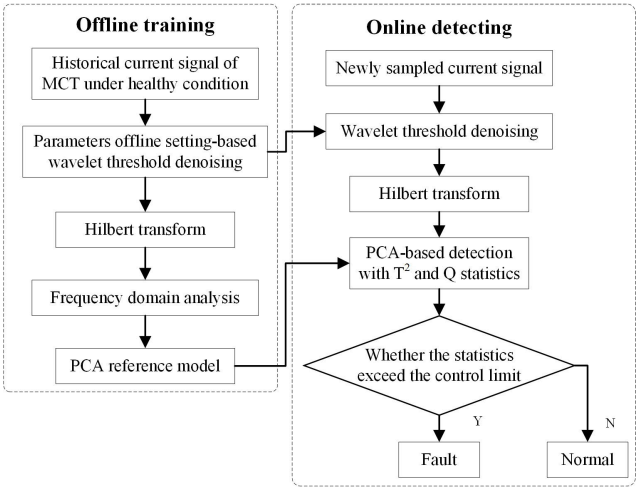

FIGURE 4. The flowchart of the proposed imbalance fault detection method.

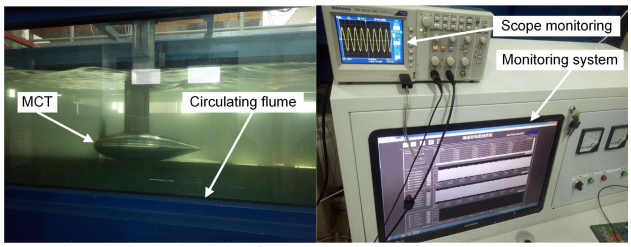

(a) The MCT in the circulating flume. (b) The monitoring system of the MCT.

FIGURE 5. The MCT experimental platform.

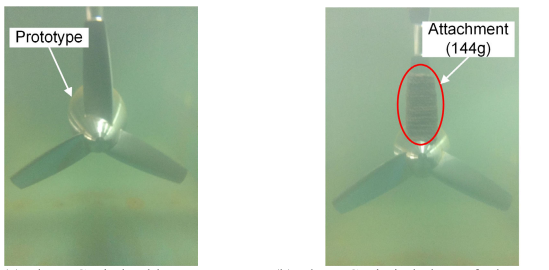

(a) The MCT in healthy state. (b) The MCT in imbalance fault state.

FIGURE 6. The imbalance fault setting of the MCT.

IV. EXPERIMENTAL RESULTS AND ANALYSIS

A. EXPERIMENTAL PLATFORM

To evaluate the effectiveness and stability of the proposed fault detection method under different flow velocity conditions, the experimental platform [18] (Fig. 5) with a 230 W direct-drive PMSG prototype (8 pole pairs) is used. As shown in Fig. 5(a), the MCT operates in a circulating flume which uses a pump motor to generate controllable flow. And this experimental platform can simulate the water environment affected by turbulence and waves. As shown in Fig. 5(b), the data acquisition and status monitoring system of the experimental platform can collect and monitor the three phase currents, voltages and flow velocity signals. The sampling frequency of the data acquisition system is 1 kHz. The blade imbalance fault is emulated by attaching winding ropes on the blade (illustrated in Fig. 6). With the experimental platform, an MCT working in the underwater environment affected by turbulence and waves can be simulated.

B. IMBALANCE FAULT DETECTION RESULTS AND ANALYSIS

1) DETECTION RESULTS AND ANALYSIS UNDER THE SAME FLOW VELOCITY CONDITION

The methods in [18], [26] and [27] mainly rely on searching the fault peak near the fault characteristic frequency to detect the imbalance fault. It is needed to manually decide whether there is an imbalance fault. To show the advantages of the proposed method, the experiments in different health states under the same flow velocity condition are carried out.

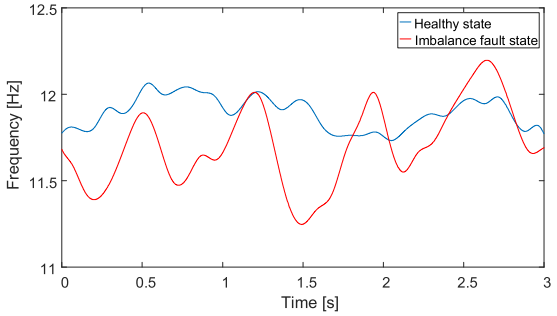

FIGURE 7. The estimated instantaneous frequencies in different health states after using the wavelet threshold denoising and HT.

In the experiment, 150 sets of the healthy stator current signals and 100 sets of the imbalance fault stator current signals under the same flow velocity conditions (1.0 m/s) are collected. The length of each set of data is 3000. 50 sets of healthy current signals were randomly selected to form the offline training data set (the data set size is 50*3000). The remaining data forms the online test data set (the data set size is 200*3000).

The frequency of the historical healthy stator current data measured from the monitoring system is around 11.7 Hz (the 1P frequency is around 1.5 Hz). With the proposed offline parameters setting method, the number of wavelet decomposition levels j is set to be 4. Coif4 and rigrsure are chosen as the wavelet basis function and the threshold selection function, respectively. With the wavelet threshold denoising and HT, the instantaneous frequency can be estimated (shown in Fig. 7). It can be seen from Fig. 7 that the vibration amplitude of the instantaneous frequency in the imbalance fault state is much larger than that in the healthy state. Therefore, the imbalance fault can be detected in time-frequency domain.

After the frequency domain analysis of the instantaneous frequency signals, the frequency domain signals are taken as inputs to the PCA for offline training. With PCA, a reference model is established. In the PCA modeling, the contribution rate of PCs is set to be 95%. The imbalance fault can be detected by comparing the statistics with the control limits calculated during the offline training. The detection results with T^2 statistic and Q statistic using the proposed method are shown in Fig. 8. With the Q statistic, the proposed method can get good imbalance fault detection results. The false alarm rate is 5.5% and the rate of missed detection is 0%. With the proposed method, the imbalance fault can be detected automatically.

2) DETECTION RESULTS AND ANALYSIS UNDER DIFFERENT FLOW VELOCITY CONDITIONS

To verify the stability of the proposed method under different flow velocity conditions, 150 sets of the healthy stator current signals and 100 sets of the imbalance fault stator current signals under different flow velocity conditions (1.0 m/s, 1.1 m/s, 1.2 m/s, 1.3 m/s, 1.4 m/s) are collected. The length

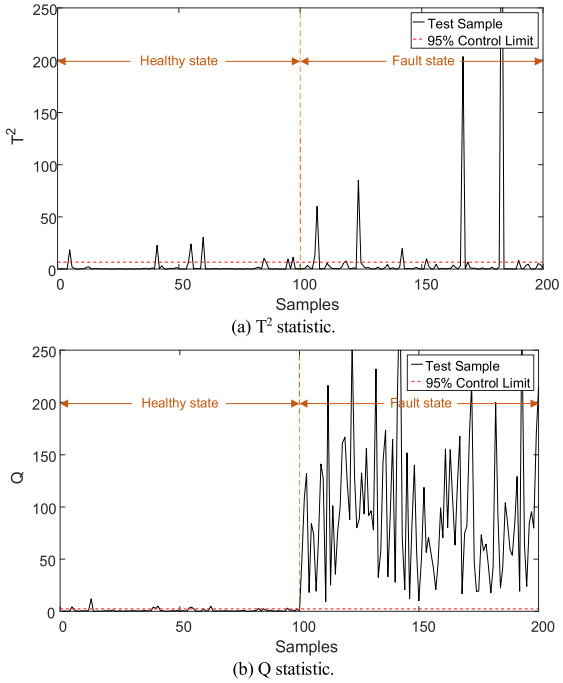

FIGURE 8. Experimental fault detection results of the proposed method under the same flow velocity condition.

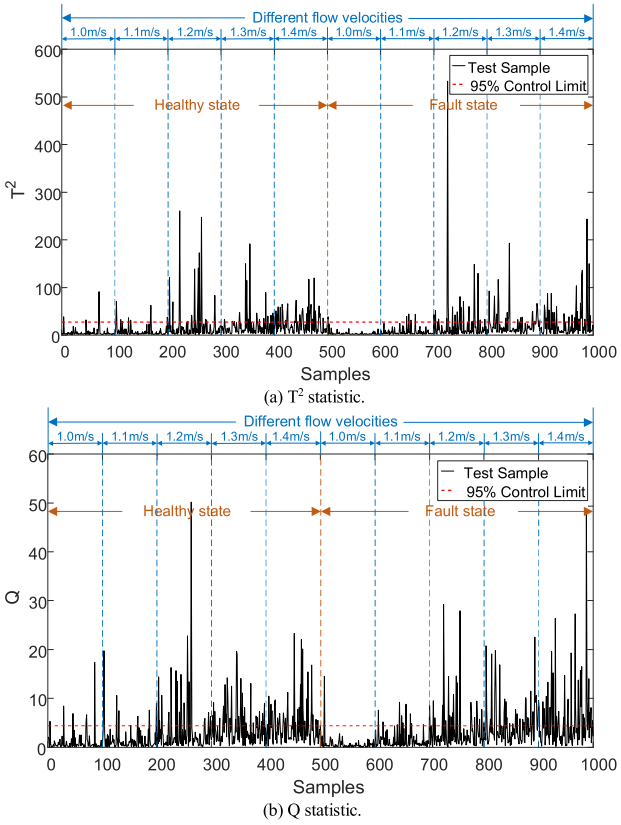

FIGURE 9. Experimental fault detection results of the method without denoising under different flow velocity conditions.

of each set of data is 3000. 50 sets of healthy current signals under different flow velocity conditions were randomly selected to form the offline training data set (the data set size

TABLE 3. The flow velocity conditions and health states of samples.

Samples	1-100	101-200	201-300	301-400	401-500	501-600	601-700	701-800	801-900	901-1000
Velocity condition	1.0 m/s	1.1 m/s	1.2 m/s	1.3 m/s	1.4 m/s	1.0 m/s	1.1 m/s	1.2 m/s	1.3 m/s	1.4 m/s
Health state	Healthy state					Fault state				

TABLE 4. Experimental fault detection results under 95% control limit.

	Method without denoising		Method using EMD		Method using moving average filter		Proposed method	
Detection index	T^2	Q	T^2	Q	T^2	Q	T^2	Q
False negative rate	42.1%	39.3%	46.1%	39.4%	44.8%	40.2%	46.9%	4.6%
False alarm rate	8.4%	10.1%	5.8%	11.9%	5.6%	11.7%	0.5%	0.8%

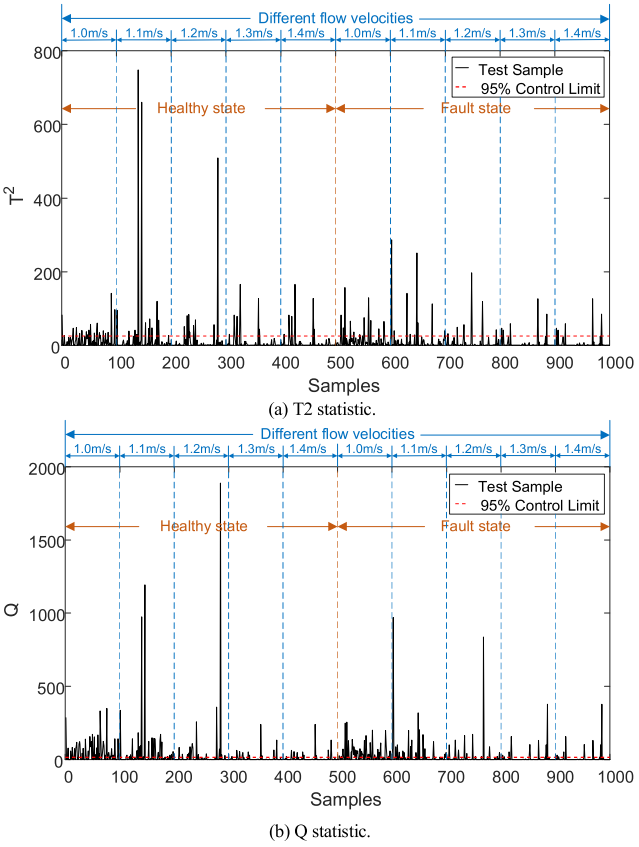

(a) T2 statistic.

(b) Q statistic.

FIGURE 10. Experimental fault detection results of the method using EMD under different flow velocity conditions.

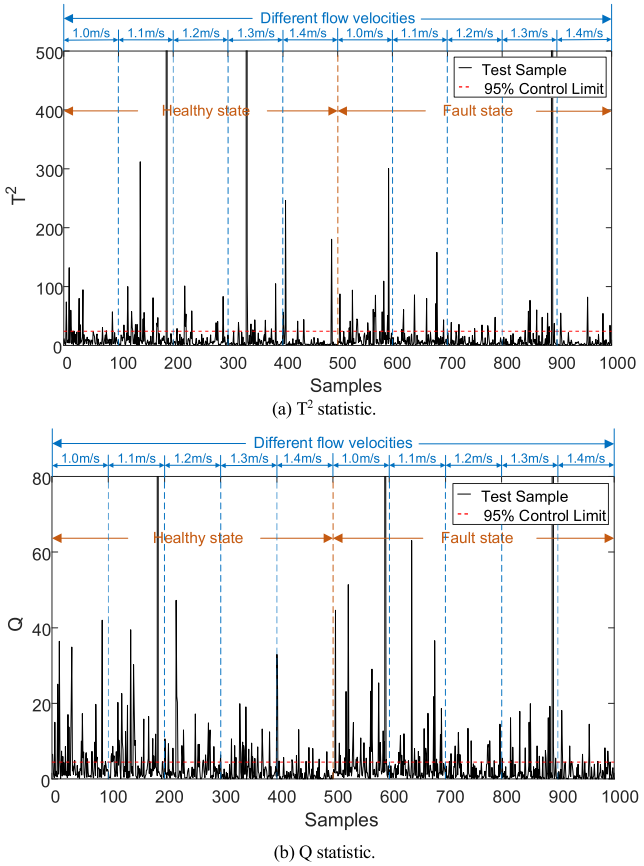

(a) T^2 statistic.

(b) Q statistic.

FIGURE 11. Experimental fault detection results of the method using moving average filter under different flow velocity conditions.

is 250*3000). The remaining data forms the online test data set (the data set size is 1000*3000).

The frequency range of the historical healthy stator current data measured from the monitoring system is 10-16 Hz (the range of 1P frequency is 1.25-2 Hz). With the proposed offline parameters setting method, the number of wavelet decomposition levels j is set to be 4. Coif4 and rigrsure are chosen as the wavelet basis function and the threshold selection function, respectively. In the PCA modeling, the contribution rate of PCs is set to be 95%. Three other methods are compared with the proposed method: one method without denoising, one method using EMD and the last one using moving average filter. To show the advantages of the proposed method, the methods mentioned above are identical except the denoising part.

Fig. 9, 10, 11 and 12 compare the detection results under different flow velocity conditions with four different methods: the method without denoising, the method using EMD, the method using moving average filter and the proposed method (the first 500 samples in healthy state and the last 500 samples in fault state. The flow velocity conditions and health states of samples are shown in Table 3). Table 4 shows

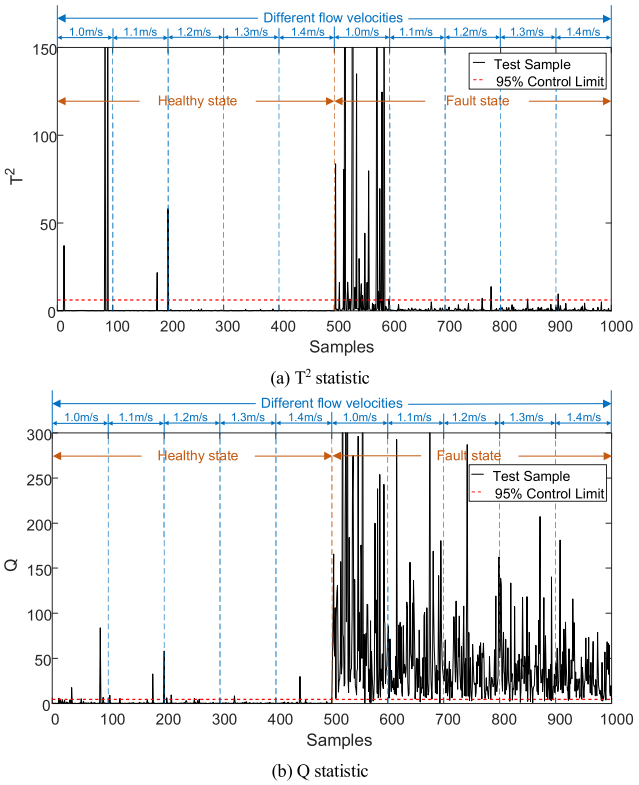

FIGURE 12. Experimental fault detection results of the proposed method under different flow velocity conditions.

the numerical results. Fig. 9 shows the imbalance fault detection results with T^2 statistic and Q statistic using the method without denoising. From Fig. 9, the detection performance is not satisfactory with regard to fault detection expectations, and both the false negative rate and the false alarm rate are too high. Fig. 10 shows the imbalance fault detection results with T^2 statistic and Q statistic with the method using EMD. The experimental results show that the false alarm rate of T^2 statistic gets lower, but the false negative rate is too high for the fault detection. Fig. 11 shows the imbalance fault detection results with the method using moving average filter. The false alarm rate of T^2 statistic can approximately meet the requirement of fault detection, but the false negative rate is still too high. Fig. 12 shows the imbalance fault detection results with the proposed method. The fault detection performances using T^2 statistic are not good. In fact, despite a low false alarm rate, the number of non-detected samples is too high to be acceptable. However, the results with the Q statistic are much better and meet the usual requirements of fault detection. The false alarm rate is less than 1% (where 5% is generally acceptable) and the rate of missed detection is less than 5%. The experimental results show that the proposed method has better stability than the existing methods mentioned above.

V. CONCLUSION

In this paper, a non-intrusive method using the generator's stator current is proposed to detect the imbalance fault in marine current turbines. At first, to deal with the interferences caused by turbulence and waves under different flow velocity conditions, the wavelet threshold denoising is applied. Second, the stator current signal in time domain is transformed to time-frequency domain by Hilbert transform. Finally, Principle Component Analysis is used and the imbalance fault is detected by the computation of statistics indices in the principal and residual subspaces. The proposed method can automatically detect the imbalance fault and has good stability under different flow velocity conditions. The experimental results under different flow velocity conditions with Q statistic have shown satisfactory imbalance fault detection with false alarm and false negative rates less than 1% and 5% respectively.

REFERENCES

[1] Z. Ren, Y. Wang, H. Li, X. Liu, Y. Wen, and W. Li, "A coordinated planning method for micrositing of tidal current turbines and collector system optimization in tidal current farms," *IEEE Trans. Power Syst.*, vol. 34, no. 1, pp. 292–302, Jan. 2019.

[2] Y. Dai, Z. Ren, K. Wang, W. Li, Z. Li, and W. Yan, "Optimal sizing and arrangement of tidal current farm," *IEEE Trans. Sustain. Energy*, vol. 9, no. 1, pp. 168–177, Jan. 2018.

[3] O. A. L. Brutto, M. R. Barakat, S. S. Guillou, J. Thiebot, and H. Gualous, "Influence of the wake effect on electrical dynamics of commercial tidal farms: application to the alderney race (France)," *IEEE Trans. Sustain. Energy*, vol. 9, no. 1, pp. 321–332, Jan. 2018.

[4] M. R. Barakat, B. Tala-Ighil, H. Chaoui, H. Gualous, Y. Slamani, and D. Hissel, "Energetic macroscopic representation of a marine current turbine system with loss minimization control," *IEEE Trans. Sustain. Energy*, vol. 9, no. 1, pp. 106–117, Jan. 2018.

[5] S. B. Chabane, M. Alamir, M. Fiacchini, R. Riah, T. Kovaltchouk, and S. Bacha, "Electricity grid connection of a tidal farm: An active power control framework constrained to grid code requirements," *IEEE Trans. Sustain. Energy*, vol. 9, no. 4, pp. 1948–1956, Oct. 2018.

[6] Z. Li, N. Maki, T. Ida, M. Miki, and M. Izumi, "Comparative study of 1-MW PM and HTS synchronous generators for marine current turbine," *IEEE Trans. Appl. Supercond.*, vol. 28, no. 4, pp. 1–5, Jun. 2018.

[7] H.-T. Pham, J.-M. Bourgeot, and M. Benbouzid, "Fault-tolerant finite control set-model predictive control for marine current turbine applications," *IET Renew. Power Gener.*, vol. 12, no. 4, pp. 415–421, Mar. 2018.

[8] Z. Ren, H. Li, W. Li, X. Zhao, Y. Sun, T. Li, and F. Jiang, "Reliability evaluation of tidal current farm integrated generation systems considering wake effects," *IEEE Access*, vol. 6, pp. 52616–52624, 2018.

[9] W. Li, H. Zhou, H. Liu, Y. Lin, and Q. Xu, "Review on the blade design technologies of tidal current turbine," *Renew. Sustain. Energy Rev.*, vol. 63, pp. 414–422, Sep. 2016.

[10] H. Titah-Benbouzid and M. Benbouzid, "Biofouling issue on marine renewable energy converters: A state of the art review on impacts and prevention," *Int. J. Energy Convers.*, vol. 5, no. 3, p. 67, Jul. 2017.

[11] X. Sheng, S. Wan, L. Cheng, and Y. Li, "Blade aerodynamic asymmetry fault analysis and diagnosis of wind turbines with doubly fed induction generator," *J. Mech. Sci. Technol.*, vol. 31, no. 10, pp. 5011–5020, Oct. 2017.

[12] M. Zhang, T. Wang, and T. Tang, "A multi-mode process monitoring method based on mode-correlation PCA for marine current turbine," in *Proc. IEEE 11th Int. Symp. Diag. Electr. Machines, Power Electron. Drives (SDEMPED)*, Aug. 2017, pp. 286–291.

[13] H. Chen, T. Tang, N. Ait-Ahmed, M. E. H. Benbouzid, M. Machmoum, and M. E.-H. Zaim, "Attraction, challenge and current status of marine current energy," *IEEE Access*, vol. 6, pp. 12665–12685, 2018.

[14] D. Zhang, L. Qian, B. Mao, C. Huang, B. Huang, and Y. Si, "A data-driven design for fault detection of wind turbines using random forests and XGboost," *IEEE Access*, vol. 6, pp. 21020–21031, 2018.

[15] G. Jiang, P. Xie, H. He, and J. Yan, "Wind turbine fault detection using a denoising autoencoder with temporal information," *IEEE/ASME Trans. Mechatronics*, vol. 23, no. 1, pp. 89–100, Feb. 2018.

[16] T. Wang, J. Qi, H. Xu, Y. Wang, L. Liu, and D. Gao, "Fault diagnosis method based on FFT-RPCA-SVM for cascaded-multilevel inverter," *ISA Trans.*, vol. 60, pp. 156–163, Jan. 2016.
[17] H. Malik and S. Mishra, "Artificial neural network and empirical mode decomposition based imbalance fault diagnosis of wind turbine using TurbSim, FAST and Simulink," *IET Renew. Power Gener.*, vol. 11, no. 6, pp. 889–902, May 2017.
[18] M. Zhang, T. Wang, and T. Tang, "An imbalance fault detection method based on data normalization and EMD for marine current turbines," *ISA Trans.*, vol. 68, pp. 302–312, May 2017.
[19] H. Malik and S. Mishra, "Proximal support vector machine (PSVM) based imbalance fault diagnosis of wind turbine using generator current signals," *Energy Procedia*, vol. 90, pp. 593–603, Dec. 2016.
[20] M. Zhang, T. Wang, T. Tang, M. Benbouzid, and D. Diallo, "Imbalance fault detection of marine current turbine under condition of wave and turbulence," in *Proc. 42nd Annu. Conf. IEEE Ind. Electron. Soc. (IECON)*, Oct. 2016, pp. 6353–6358.
[21] S. Golestan, M. Ramezani, J. M. Guerrero, and M. Monfared, "dq-frame cascaded delayed signal cancellation- based PLL: Analysis, design, and comparison with moving average filter-based PLL," *IEEE Trans. Power Electron.*, vol. 30, no. 3, pp. 1618–1632, Mar. 2015.
[22] Y. Amirat, M. Benbouzid, T. Wang, K. Bacha, and G. Feld, "EEMD-based notch filter for induction machine bearing faults detection," *Appl. Acoust.*, vol. 133, pp. 202–209, Apr. 2018.
[23] W. Fan, Q. Zhou, J. Li, and Z. Zhu, "A wavelet-based statistical approach for monitoring and diagnosis of compound faults with application to rolling bearings," *IEEE Trans. Autom. Sci. Eng.*, vol. 15, no. 4, pp. 1563–1572, Oct. 2018.
[24] Z. Geng, J. Chen, and Y. Han, "Energy efficiency prediction based on PCA-FRBF model: A case study of ethylene industries," *IEEE Trans. Syst., Man, Cybern., Syst.*, vol. 47, no. 8, pp. 1763–1773, Aug. 2017.
[25] M. Rafferty, X. Liu, D. M. Laverty, and S. Mcloone, "Real-time multiple event detection and classification using moving window PCA," *IEEE Trans. Smart Grid*, vol. 7, no. 5, pp. 2537–2548, Sep. 2016.
[26] X. Gong and W. Qiao, "Imbalance fault detection of direct-drive wind turbines using generator current signals," *IEEE Trans. Energy Convers.*, vol. 27, no. 2, pp. 468–476, Jun. 2012.
[27] M. Zhang, T. Wang, T. Tang, Z. Liu, and C. Claramunt, "A synchronous sampling based harmonic analysis strategy for marine current turbine monitoring system under strong interference conditions," *Energies*, vol. 12, no. 11, p. 2117, Jun. 2019.
[28] H. Chen, N. Ait-Ahmed, M. Machmoum, and M. E.-H. Zaim, "Modeling and vector control of marine current energy conversion system based on doubly salient permanent magnet generator," *IEEE Trans. Sustain. Energy*, vol. 7, no. 1, pp. 409–418, Jan. 2016.
[29] H.-T. Pham, J.-M. Bourgeot, and M. E. H. Benbouzid, "Comparative investigations of sensor fault-tolerant control strategies performance for marine current turbine applications," *IEEE J. Ocean. Eng.*, vol. 43, no. 4, pp. 1024–1036, Oct. 2018.
[30] X. Gong and W. Qiao, "Bearing fault diagnosis for direct-drive wind turbines via current-demodulated signals," *IEEE Trans. Ind. Electron.*, vol. 60, no. 8, pp. 3419–3428, Apr. 2013.
[31] Z. Liu, Z. He, W. Guo, and Z. Tang, "A hybrid fault diagnosis method based on second generation wavelet de-noising and local mean decomposition for rotating machinery," *ISA Trans.*, vol. 61, pp. 211–220, Mar. 2016.
[32] A. Bhandari, D. Kumar, A. Kumar, and G. Singh, "Optimal sub-band adaptive thresholding based edge preserved satellite image denoising using adaptive differential evolution algorithm," *Neurocomputing*, vol. 174, pp. 698–721, Jan. 2016.
[33] H.-T. Chiang, Y.-Y. Hsieh, S.-W. Fu, K.-H. Hung, Y. Tsao, and S.-Y. Chien, "Noise reduction in ECG signals using fully convolutional denoising autoencoders," *IEEE Access*, vol. 7, pp. 60806–60813, 2019.
[34] E. Elbouchikhi, V. Choqueuse, Y. Amirat, M. El Hachemi Benbouzid, and S. Turri, "An efficient Hilbert–Huang transform-based bearing faults detection in induction machines," *IEEE Trans. Energy Convers.*, vol. 32, no. 2, pp. 401–413, Jun. 2017.
[35] M. Z. Sheriff, M. Mansouri, M. N. Karim, H. Nounou, and M. Nounou, "Fault detection using multiscale PCA-based moving window GLRT," *J. Process Control*, vol. 54, pp. 47–64, Jun. 2017.
[36] M. Mansouri, M. Z. Sheriff, and R. Baklouti, "Statistical fault detection of chemical process-comparative studies," *J. Chem. Eng. Process Technol.*, vol. 7, no. 1, pp. 282–291, 2016.

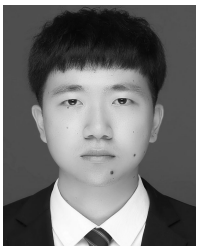

ZHICHAO LI received the B.S. degree in ship electronic and electrical engineering from Shanghai Maritime University, Shanghai, China, in 2017, where he is currently pursuing the M.S. degree in electric engineering.

TIANZHEN WANG (Senior Member, IEEE) was born in Qingdao, China, in 1978. She received the B.S. degree in industrial automation from the Shandong University of Technology, Shandong, China, in 2001, and the Ph.D. degree in power electronics and power drive from Shanghai Maritime University, Shanghai, China, in 2006.

Since 2016, she has been both a Research Affiliate and Doctoral Supervisor of the Institut de Recherche Dupuy de Lôme (IRDL) with the University of Brest, and a Professor and Doctoral Supervisor with the Department of Electrical and Automation, Shanghai Maritime University. She is a Full Professor with Shanghai Maritime University. Her research interests include fault diagnosis, and fault tolerant control methods and its applications in inverters, wind power generators, and ocean current machine.

Prof. Tianzhen awards and honors include a Committee Member of fault diagnosis and safety on the Technical Process Specialized Committee, and the Cognitive Computing and System Specialized Committee China Automation Society.

YIDE WANG (Senior Member, IEEE) received the B.S. degree in electrical engineering from the Beijing University of Posts and Telecommunications, Beijing, China, in 1985, and the M.S. and Ph.D. degrees in signal processing and telecommunications from the University of Rennes, France, in 1986 and 1989, respectively. His research interests include array signal processing, spectral analysis, and mobile wireless communication systems.

YASSINE AMIRAT (Senior Member, IEEE) was born in Annaba, Algeria, in 1970. He received the B.Sc. and M.Sc. degrees in electrical engineering from the University of Annaba, Annaba, in 1994 and 1997, respectively, and the Ph.D. degree in wind turbine condition monitoring from the University of Brest, Brest, France, in 2011.

He was a Lecturer with Annaba University, from 2000 to 2010. He is currently an Associate Professor of electrical engineering with ISEN, Brest. He is also an Affiliated Member of the CNRS, UMR, Institut de Recherche Dupuy de Lôme(IRDL). His main research interests include electrical machines faults detection and diagnosis, fault tolerant control, and signal processing and statistics for power systems monitoring. He is also interested in renewable energy applications such as wind turbines, marine current turbines, and hybrid generation systems.

MOHAMED BENBOUZID (Fellow, IEEE) received the B.Sc. degree in electrical engineering from the University of Batna, Batna, Algeria, in 1990, and the M.Sc. and Ph.D. degrees in electrical and computer engineering from the National Polytechnic Institute of Grenoble, Grenoble, France, in 1991 and 1994, respectively, and the Habilitation à Diriger des Recherches degree from the University of Picardie Jules Verne, Amiens, France, in 2000.

After receiving the Ph.D. degree, he joined the Professional Institute of Amiens, University of Picardie Jules Verne, where he was an Associate Professor of electrical and computer engineering. Since September 2004, he has been with the University of Brest, Brest, France, where he is currently a Full Professor of electrical engineering. He is also a Distinguished Professor and a 1000 Talent Expert with Shanghai Maritime University, Shanghai, China. His main research interests and experience include analysis, design, and control of electric machines, variable-speed drives for traction, propulsion, and renewable energy applications, and fault diagnosis of electric machines.

Prof. Benbouzid has been elevated as an IEEE Fellow for his contributions to diagnosis and fault-tolerant control of electric machines and drives. He is also a Fellow of the IET. He is the Editor-in-Chief of the *International Journal on Energy Conversion* and *Applied Sciences* (MDPI), a section on electrical, electronics, and communications engineering. He is a Subject Editor of the *IET Renewable Power Generation*. He is also an Associate Editor of the IEEE TRANSACTIONS ON ENERGY CONVERSION.

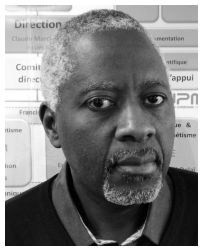

DEMBA DIALLO (Senior Member, IEEE) received the M.Sc. and Ph.D. degrees in electrical and computer engineering from the National Polytechnic Institute of Grenoble, France, in 1990 and 1993, respectively. He is currently a Full Professor with University Paris-Sud and the Director of the French National Research Network on Electrical Engineering. He is with the Group of Electrical Engineering Paris, France. His current areas of research include fault diagnosis, fault tolerant control, and energy management. The applications of his research are related to more electrified transportation systems and microgrids with renewable energies.